

# The CFD Analysis of a CI Engine's Combustion Properties as it Runs on Chicken Fat Biodiesel at Various Compression Ratios

Rajeesh S.<sup>1</sup>, Hemavathy S.<sup>2</sup>, T. Anil Kumar<sup>3</sup> Ravi K. M<sup>4</sup>, Aradhya S. M.<sup>5</sup>

<sup>1</sup>Assistant Professor, Department of Mechanical Engineering, Ramaiah Institute of Technology, Bengaluru, Karnataka, India

<sup>2</sup>Assistant Professor, Department of Industrial Engineering and Management, Ramaiah Institute of Technology, Bengaluru, Karnataka, India

<sup>3</sup>Associate Professor, Department of Mechanical Engineering, Ramaiah Institute of Technology, Bengaluru, Karnataka, India

<sup>4</sup>Assistant Professor, Department of Mathematics, R V College of Engineering, Bengaluru, Karnataka, India

<sup>5</sup>Assistant Professor, Department of Mechanical Engineering, Kalpataru Institute of Technology, Tiptur, Karnataka, India.

**Abstract:** In this research, the properties of combustion in a 4-Stroke compression ignition (CI) Kirloskar engine that burns a mixture of diesel fuel and 20% biodiesel (CB20) made from chicken fat are studied experimentally and numerically. Three nozzles with a 0.15mm diameter are used to inject the fuel into the Kirloskar 4 stroke diesel engine's cylinder at a pressure of 220 bar. As the compression ratio increases, BP, BTE, and emissions of CO increased and decreased in the BSFC, Carbon dioxide and emissions of HC. The best emission characteristics are found in CB20, which performs better than all biodiesel blends at full load (80%). Through experimentation, it was possible to determine parameters like as combustion characteristics, peak pressures that were created, and corresponding changes in cylinder volume during the compression and expansion strokes relative to piston movement. The volume, pressure, quantity of heat emitted during fuel combustion, and temperature in the IC engine cylinder are all monitored by IC engine model as a simulation tool in the ANSYS software. The simulation's peak pressure, volume, heat release rate, and temperature variations are compared to the corresponding experimental data for CR 14:1, 16.5:1, and 18:1, without modification in the CI engine. As a consequence, CFD study may prove useful to future combustion modelling researchers.

**Keywords:** CFD, biodiesel from Chicken fat, Characteristics of Combustion, Kirloskar 4 stroke diesel engine, VCR.

## Nomenclature

CCs	Combustion characteristics	CA	Crank angle	
CI	Compression Ignition	BTDC	Before top dead center	
CB20	20% chicken fat biodiesel by volume blended to diesel fuel	ATDC	After top dead center	VCR
			Variable compression ratio	
CRs	Compression ratios	ABDC	After bottom dead center	
IC	Internal combustion	BBDC	Before bottom dead center	
CFD	Computational Fluid Dynamics	EVO	Exhaust Valve open	
NOx	Nitrogen oxides	IVC	Inlet valve close	
TDC	Top dead center	HRR	Heat release rate	

## 1. Introduction

In numerous industries, as well as in the current condition of automobiles, there is an increasing demand for diesel, but the high compression ratio is also creating pollutants in the environment. Combining biodiesel with diesel fuel can improve the engine's efficiency and emissions characteristics. Optimum biodiesel blends can significantly lower fuel dependence and pollution without modifying diesel engines<sup>1</sup>. Biodiesel is made from natural resources and has a number of advantages for the environment. The concentration of oxygen of biodiesel decreases carbon monoxide and hydrocarbon emissions while boosting NOx emission<sup>2</sup>.

The cost of the necessary measuring devices is significant, and studying comprehensive combustion and emission data takes additional time. As a result, CFD (Computational fluid dynamics) analysis plays a critical role in accurately predicting simulation results through adequate modelling. Physical and chemical features of biodiesel: specific heat, Density, viscosity, thermal conductivity, latent heat, boiling point, and other factors all have an impact on fuel spray and combustion modelling, improving the precision of numerical CCs parameter prediction.

L. Lenik et al.<sup>3</sup> discussed the sub models that used fresh observational data and AVL programming to predict the ignition model's boundaries. An increased mix percentage has decreased start postponement, force, and motor result by lowering the calorific value of the fuel. Exploratory and mathematical calculations indicate a 10% variation in in-chamber pressure for 2000rpm.

S M Karishma et al.<sup>4</sup> tested the performance of a diesel-aricot biodiesel blend using a single-cylinder, four-stroke, water-cooled engine. It was discovered that mixing 20% apricot oil with biodiesel improves performance while lowering attribute emissions when compared to other mixing ratios.

R Upendra et al.<sup>5,6</sup> and K Narendra et al.<sup>7</sup> examine the performance and emissions of a diesel engine using a blend of biodiesel and diesel fuel through numerical analysis. Nozzle opening pressure (NOP) was modified to 220 bar and injection timing was accelerated (23.5 ° B TDC) at half load and 100% load.

To enhance combustion parameters, P. R. Ganji et al.<sup>8</sup> employ response surface techniques and the CONVERGE ICS simulation tool. The fuel parameters of the major kind of ester contained in biodiesel were used to model turbulence, fuel spray, and combustion.

Edwin et al.<sup>9</sup> investigated "the thermophysical properties of several oils and developed correlations that predict their qualities across a wide temperature range. The statistical analysis of temperatures between 299.15 and 433.15 K was evaluated using the coefficient of determination, residual analysis, and significance level. The maximum thermal conductivities and heat capacities were found in the fatty acid compositions of miristic, palmitic, stearic, oleic, linoleic, and linolenic acids".

To determine how injection pressure impacts CI motors, Anuradha.C et al.<sup>10</sup> conducted a CFD simulation. Estimates of mass flow and velocity were made for three distinct injection pressures of 150, 200, and 250 bars for the combustion experiment using the 45° area model. Replicated results using the STAR-CD system revealed an increase in chamber strain, temperature, and HRR when injection pressure was increased.

Ansys FLUENT was used to observe the combustion of Thumba biodiesel in CI engine by Rajesh G et al.<sup>11</sup>. The limited number of species that can be used for biodiesel replacement oxidation was discussed, as well as a lack of chemical kinetics mechanisms to produce appropriate simulation results. The fatty acid composition of biodiesel was used to establish the fuel parameters for the simulation. Three 0.15mm-diameter nozzles were employed with a 30° injector angle to the vertical. To examine the effects of grid independence on the combustion parameters of volume, pressure, temperature and Heat release rate at inside the cylinder, the fuel was injected at 23° crank angle before top dead centre and 7° crank angle after top dead centre. The experimental and computational results showed a similar tendency, with HRR starting 2 to 3° earlier for biodiesel than diesel fuel at a CA. During combustion, biodiesel was expected to have higher temperatures and pressures than diesel. It was also revealed that when the blending ratio increases, cylinder pressure increases.

The CFD code FLUENT tool was used by Umakant K et al.<sup>12</sup> to validate the combustion of a diesel direct-injection engine. As a result of the RNG k-model turbulence in the cylinder, 66.16 bar was the maximum pressure for modelling. Whereas the maximum pressure for CFD was 63.55 bar, which was similar with CA 3660 experimental data. In modelling, the heat release rate at CA 364° operating at full load is 79.0 Joules per degree, whereas in experiment, it is 77.34 Joules per degree.

Ajay Kolhe et al.<sup>13</sup> used CFD to predict combustion in a CI engine running on pongamia biodiesel. The RNG k-model was utilized to account for the influence of turbulence using the CFD commercial tool FLUENT. “To predict the characteristics of the combustion inside the cylinder, models of chemistry rate end products and species transit were used to model the spray, droplet collisions, and sub-models utilising Taylor-Analogy Breakup (TAB). The findings of the modelling were identical to those of the experiments, although with higher values”.

Several studies were conducted to mimic combustion chambers using various CFD codes that were available. The majority of researchers employed 20 percent biodiesel by volume in their investigations, according to the literature, it possesses characteristics that are both chemically and physically similar to those of diesel fuel. Additionally, there was acceptable percentage variance in the results when comparing the combustion parameters between the experimental and numerical methods. In order to investigate how combustion properties, respond in the four-stroke single cylinder Kirloskar VCR engine at 83.3 % engine load, this research includes an experiment analysis of diesel engine CCs using CB20 fuel for three different CRs: 14, 16.5, and 18. The results are validated with CFD analysis.

## 2. Materials and Methods

A blend of diesel fuel and 20 percent biodiesel derived from chicken fat (CB20) was employed for the experimental CCs assessment. The engine was run at a constant speed to assess the characteristics of the CCs for three different CRs: 14, 16.5, and 18. The properties of CB20 biodiesels based on a biodiesel fatty acid composition test's % peak area are shown in Table 1<sup>14,15</sup>

**Table 1. CB20 fuel Properties**

biodiesel Properties	CB20	Biodiesel Properties	CB20
Density (kg/m <sup>3</sup> )	854	Thermal conductivity (w/m-k)	0.164
Viscosity (kg/m-s)	0.003	Heat Value (j/kg-k)	2076
Calorific value (kJ/kg)	42375	Boiling point (K)	484
Latent heat (j/kg)	269600		

Oleic acid made up roughly 40.78 percent of the biodiesel in this investigation, and CB20 properties were assessed at 300 K<sup>16</sup>. Table 2 displays the specifications of the single-cylinder, four-stroke cc engine. At a constant speed of 1500 rpm, variable loads for various fuels were assessed. Maximum pressure, volume rated for CB20 biodiesel at CR 14:1, 16.5:1, and 18:1 correspondingly. Figure 1 illustrates the flow diagram for the engine testing for various CRs. An ISO 3046-3:2006 standard water-cooled, single-cylinder, 4-stroke, stationary, and constant-speed diesel vertical engine coupled to an eddy current dynamometer experimental test rig was used for the tests at the CI engine laboratory (Mechtrix engineers Pvt Ltd, Bangalore, India). The data collection system also includes the lubrication system, fuel system, and several sensors and meters to monitor exhaust gas temperature, load, and air and fuel flow. Thermal performance and engine emission components may be evaluated using this arrangement. BP, SFC, and Exhaust temperature are the key performance indicators. The configuration also includes the exhaust gas analyzer. Using an exhaust gas analyzer, the exhaust gas constituents like CO, HC, and NOx are analysed.

**Table 2. Engine Details**

Parameters	Specification	Parameters	Specification
Type	Kirloskar - AV1	closing of Inlet valve	35.5° ABDC
Cylinder bore diameter	80 mm	opening of Exhaust valve	35.5° BBDC

Stroke length	110 mm	Injector nozzles	3 Nos
Swept Volume	552 cc	diameter of Injector nozzle	0.15 mm
Connecting rod length	234 mm	Injector pressure, bar	220
Load indicator	Digital, load : 0-50 Kg, 230V AC Supply	Exhaust gas analyzer	Make – Smart cap Technologies, Five gas analyzer
Temperature sensor	Type RTD, PT100 and Thermocouple, Type K	Load sensor	Load cell, type strain gauge, range 0-50 Kg
Dynamometer	Type eddy current, water cooled, with loading unit	Crank angle sensor	Resolution 1 Degree, Speed 5500 rpm with TDC pulse.

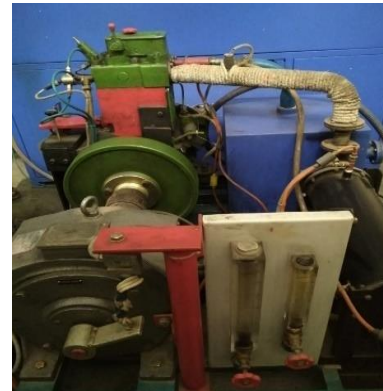
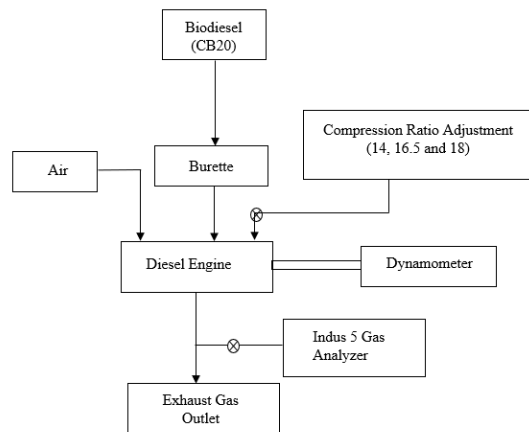


Figure 1. Experimental Set Up in Diesel Engine

### 3. CFD Analysis Process

In this research, work in cylinder combustion CFD simulation was carried out. The ANSYS fluent software IC engine workbench was selected for combustion simulation. The steps involved in Combustion simulation of IC engine as per software are shown in Figure .

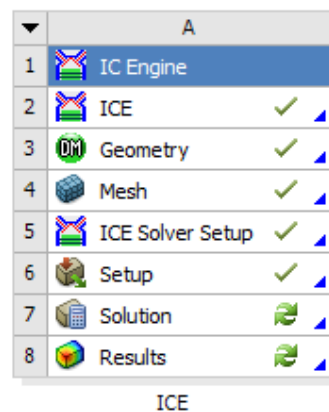


Figure 2: Steps involved in combustion simulation of IC engine as per software

The above mentioned steps were carried out for combustion simulation of CI engine fueled with neem biodiesel (20 % Chicken fat biooil blended with 80% diesel) at compression ratio 14:1 are explained below.

1. Selection of work bench and nameing of project: In this step IC engine workbench of ANSYS fluent software was selected.
2. Input of IC engine Specification and Selection of type of combustion simulation: In this section, stroke length, Length of connecting, length of crank, engine speed, crank angle at which Inlet & outlet valves opens and closes etc were input according to the engine specification and combustion simlation type was selected as shown in figure 3.

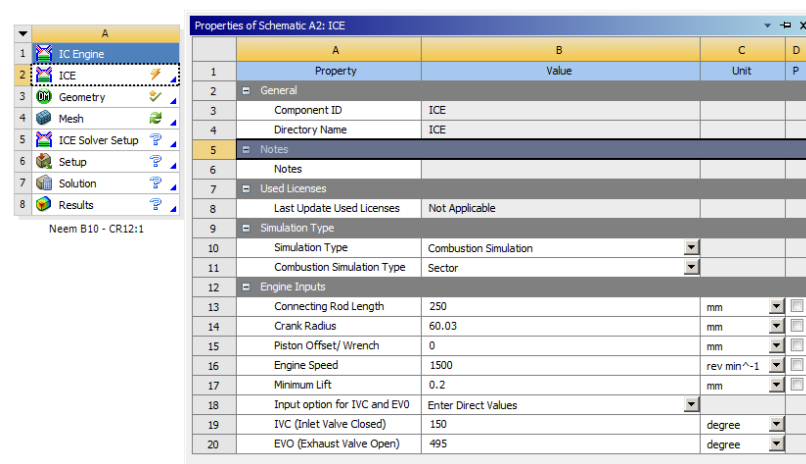
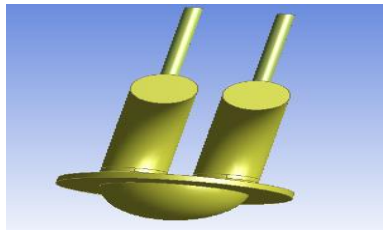


Figure 3: Input of IC engine Specification and Selection of type of combustion simulation

3. Creation of IC engine geometry and location of fuel injector.
4. The IC engine parts, such as inlet valve, exhaust valve, cylinder and piston part modelling were done as per engine specifications and assembed as one unit. The three nozzles with a hole diameter of 0.35 mm were used in the injection system with difference of  $120^\circ$ , kept at  $70^\circ$  and 0.02mm from the center of the head of the cylinder as shown in **Error! Reference source not found.**



Part Drawing of IC engine shows inlet valve, exhaust valve, cylinder and type of piston

Name	InputManager1
Sector Decomposition Type	Complete Geometry
Cylinder Faces	1 Face
Sector Angle	120 °
Spray Location Option	Height and Radius
Spray Location, Height	0.02 mm
Spray Location, Radius	0.02 mm
Spray Angle	70 °
Validate Compression Ratio	Yes
Compression Ratio	12

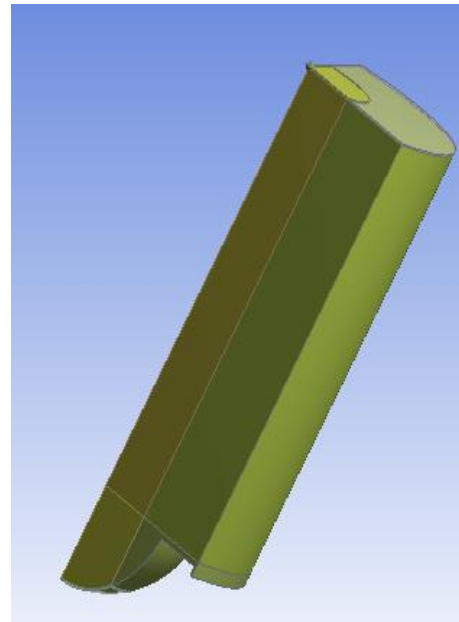


**Figure Error! No text of specified style in document.: Geometry and Details of fuel injector.**

**Figure 5: 120° Decomposed IC engine**

The three nozzles were kept at 120° difference, so the part modeling of IC engine needed to be decompose to 120° angle as shown in Figure For accurate simulation of combustion of fuel injected by one injector.

5. Meshing of decomposed IC engine part: The automatic sector meshing was carried out with meshing size conditions as shown in Figure 6.

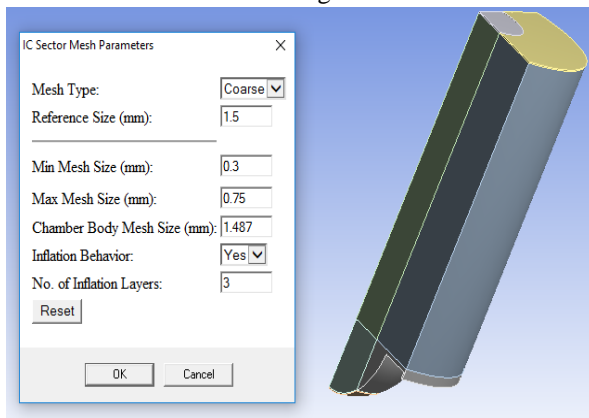


**Figure 6: 120° decomposed IC engine before meshing with meshing size conditions**

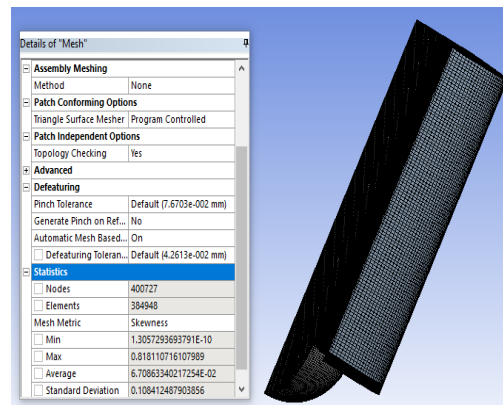


**Figure 7: 120° decomposed IC engine after meshing with meshing result**

During the mesing process the decomposed IC engine pats divided into 400727 nodes and 384948 elemnets with a maximum skewness of 0.818 as shown in Figure 7.

6. Setting up the simulation by Space discretization and Time discretization

After the demcomposed geometry was meshed properly, the simulation set up was carried out by proper input to the basic settings, physical conditions, boundry conditions, monitor definitions, initialization and solution control of simulation. In the basic setting, the number of crank angle to run for simulation of compression and power stroke were automatically calculated by the software based on the input given for inlet valve closes and

exhaust valve opens. In the physical setting, the injection properties were set up based on the engine specification, such as position of injector (along X, Y & Z axis), angle of injector, crank angle for start & end of injection, tempreature of injected fuel and velocity is shown in Figure 8.

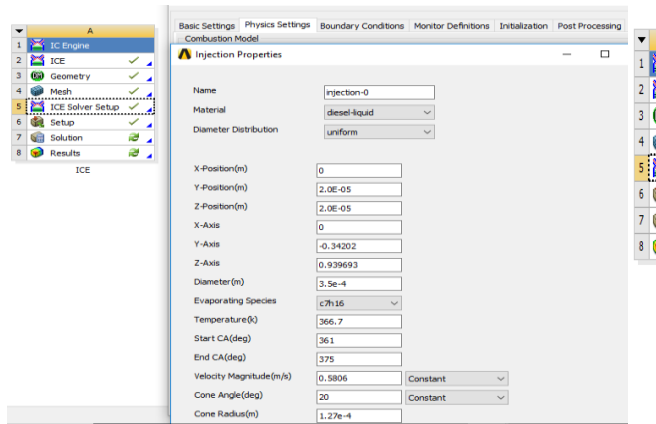


Figure 8: Setting up of fuel injection properties

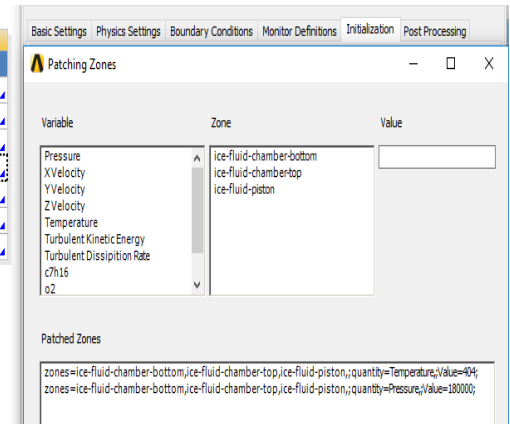


Figure 9: Setting up of combustion chamber temperature and pressure

In the initialization setup, the combustion chamber tempreture and pressure were set as 404 K and 180 bar resepctively as shown in Figure 9. In the post processing setup, the different images were setup to carryout different simulation result analysis at different crank angle.sample seeting is shown in Figure 10.

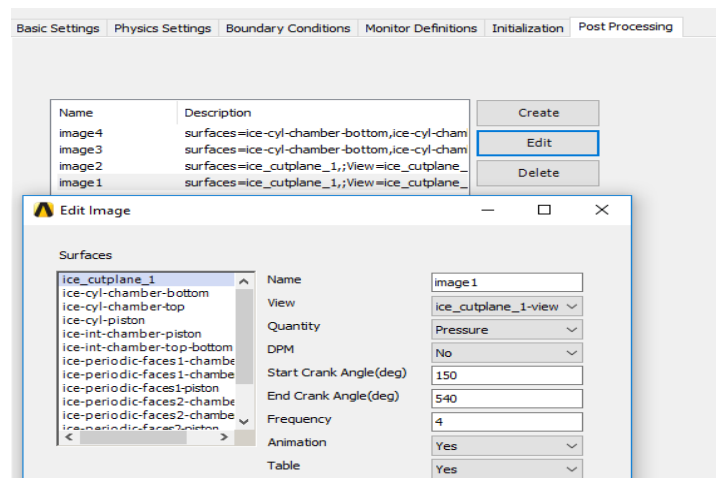


Figure 10: Setting up of different images for different simulation analysis

## 6. Running the solution

In this step three dimensional simulation run was started with double precision for accurate result and in parallel with increased number of processors to complete the solution in less time. The simulation were launch with certain setting as shown in Figure 11, and set for 1980 time steps of each 50 iterations as shown in Figure12. The simulation was completed after 80 hours hours of run.



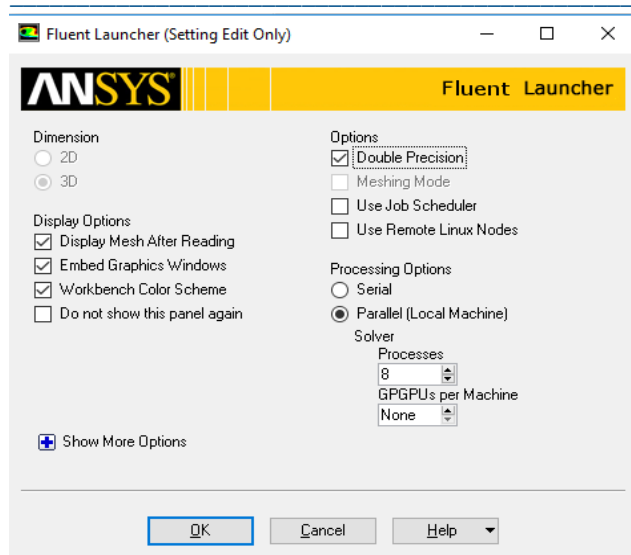


Figure 11: Running the simulation calculation by Fluent Launcher.

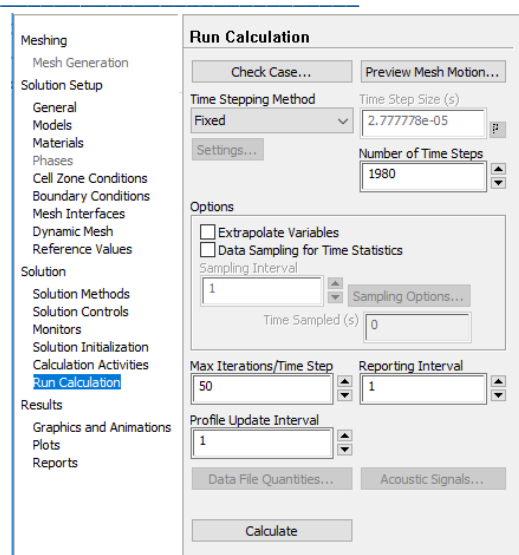


Figure 12: Setting of the number of time steps and number of iterations.

## 7. Obtaining the result.

The obtained results were tabulated and discussed in Result & discussion section.

## 4. Numerical Model Set-Up

To explore engine CCs, a 3D in-cylinder CI engine model with a 120° angle is utilised for the CFD analysis. Grid generation is carried out for three different models with CRs of 14:1, 16.5:1, and 18:1 utilising the Design Modeler ANSYS tool to produce the in-cylinder geometry.<sup>17</sup>

With a grid size of 2 mm, Figure 13 depicts the numerical CAD model for the CR 14:1, 16.5:1, and 18:1, and Table 3 lists the total components and skewness following grid building for each of the three distinct ratios. Three 0.15 mm nozzle holes are evaluated, as well as a 15° slanted sector with one hole. For the combustion chamber analysis, no valves were modelled. The piston bowl of the engine is hemispherical and is 48mm in diameter. A mass profile model of fuel injection was used, with the CA 23° BTDC and 7° ATDC fixed. A CB20-fueled CI engine was tested at a total mass flow rate of 8.7e-5 kg/s for CR 14:1, 16.5:1, and 18 to examine the volume, peak pressure, temperature, and HRR profile in the combustion chamber.

Table 3. Volume skewness and Number of elements in the grid

Compression Ratio	Volume skewness	Number of elements
14	0.83	142572
16.5	0.836	155134
18	0.847	179940

## 5. Results and Discussions

### 5.1 Engine cylinder Pressure

Figures 14 to 16 display the engine cylinder pressure for each crank angle rotation diagram for various CRs based on experimental and CFD analysis. The experimental and CFD peak pressure values for various CRs are shown in Figure 17. According to the experimental findings, CR 14, 16.5 and 18 generate maximum cylinder pressures of 54.19 bars, 65.92 bars, 71.11 bars, and 57.34 bars at crank angles of 369°, 367°, and 367° respectively. At the same crank angle of 365.7°, the CFD study shows that the peak pressures produced in the



cylinder for CR 14, 16.5 and 18 are 57.34 bars, 71.52 bars, and 82.9 bars, respectively. Results demonstrate that the CFD simulation's crank angle for the peak pressure at all CRs is unchanged. Contrarily, in an experimental examination, when the crank angle changes, the cylinder volume changes, causing multiple stages of combustion and varying ignition timings, which in turn generate different peak pressures at various crank angles for various CR. In a CFD simulation based on energy and mass conservation equations with an initial boundary condition, the characteristics of biodiesel change linearly. As the CR rises, the maximum pressure in the cylinder also rises, but the ignition delay falls<sup>18</sup>. Because there is more oxygen and more cetane in the biodiesel during the initial stages of combustion, there is a faster rate of fuel combustion. The outcome is a maximum operating pressure that is closely tied to TDC due to an increase in CR and a rise in operating temperature in the fuel. In turn, this reduces the ignition delay<sup>19,20</sup>.

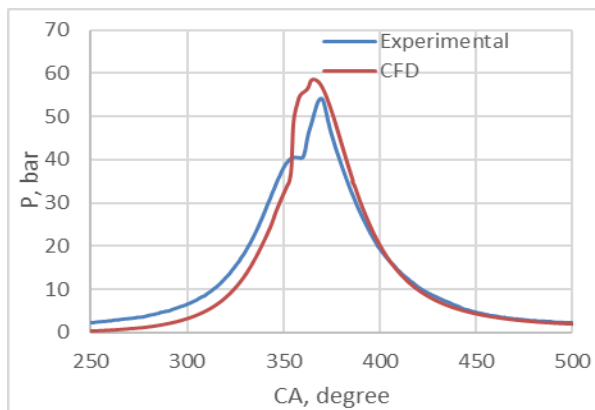


Figure 14. Pressure vs. Crank angle for CR 14

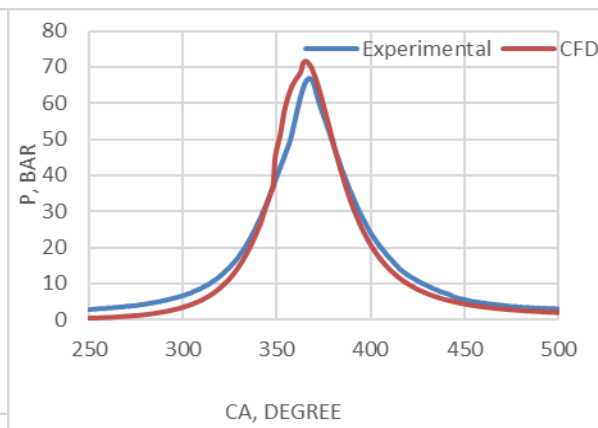


Figure 15. Pressure vs. Crank angle for CR 16.5

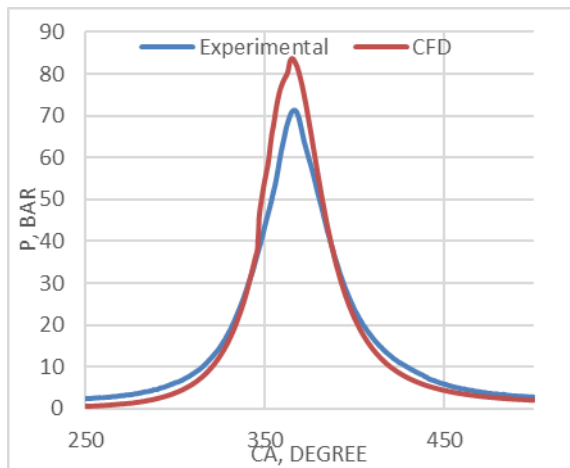


Figure 16. Pressure vs. Crank angle for CR 18

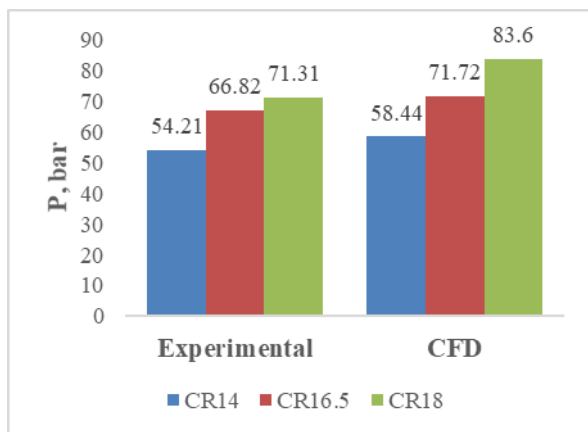


Figure 17. Peak Pressure in bar at different CR

For the Pressure vs Crank angle diagram necessary for validation, "Table 4" demonstrates the link between experimental and CFD data.

Table 4. The percentage of difference in peak pressure between experimental and CFD data

CR	% of Peak pressure difference between Experimental & CFD
14:1	7.24
16.5:1	6.83
18:1	14.7

## 5.2 cylinder pressure vs. Volume (P-V) Diagrams

As cylinder pressure increases throughout the compression stroke of a CI engine, the volume inside the cylinder is depleted until the piston top surface contacts TDC. Figures 18 through The experimental and CFD P-V diagram values for the CRs 14:1, 16.5:1, and 18:1 are shown in Figure 20. The simulated exhaust valve opening occurs before 35.5° CA during the engine's compression and expansion strokes inside the cylinder, and a slight divergence can be seen in the curve. As a result, the simulation curve continues to be open.

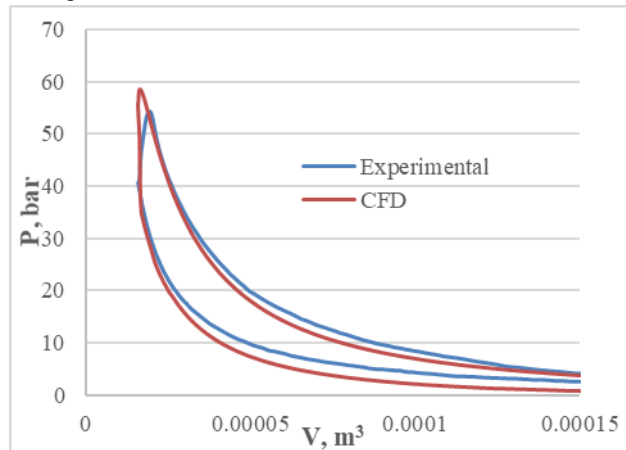


Figure 18. Pressure- Volume diagram for CR 14

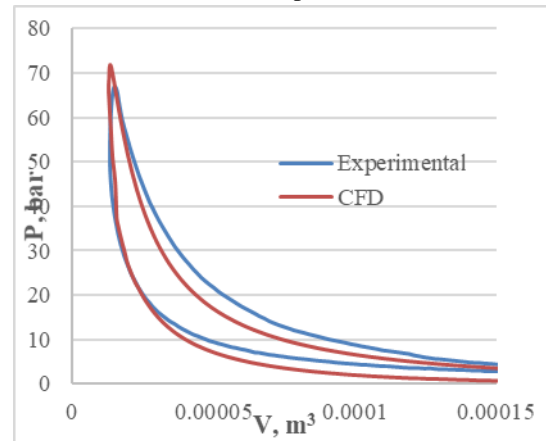


Figure 19. Pressure- Volume diagram for CR 16.5

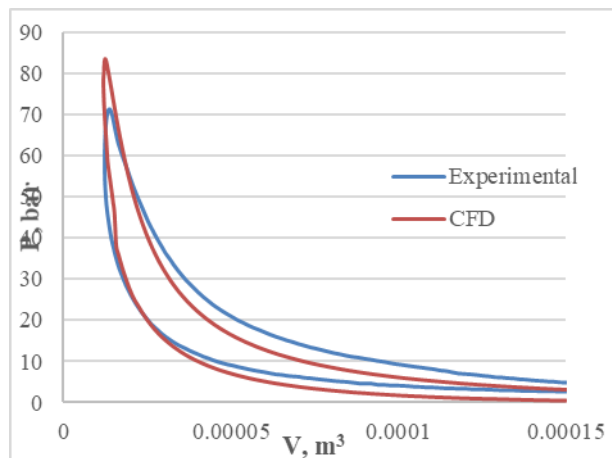


Figure 20. Pressure- Volume diagram for CR 18

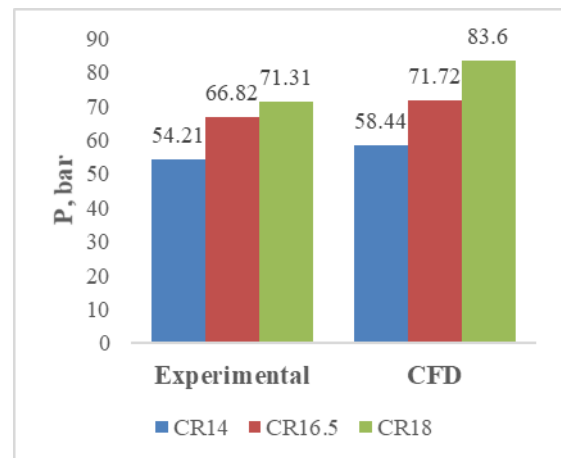


Figure 21. Pressure at different CRs

Figure 21 illustrates the measurement of the highest peak pressure inside the cylinder using both experimental and CFD analysis. When compared to experimental data, the CFD research shows the highest peak pressure with the greatest volume consumption. In the experimental example at CRs of 14:1, 16.5:1, and 18:1, this could be attributed to piston-to-cylinder leakage during the compression stroke. [21,22].

## 5.3 Heat Release Rate (HRR)

Figure 22 illustrates the predicted HRR change for the CB20 at various crank angles at varying CRs. The HRR in the cylinder is determined by a CFD analysis to be 36.33 J at 364°, 32.85 J at 364°, and 27.54 Joules at 363° crank angles for CR 14:1, 16.5:1, and 18. During the premixed combustion phase, the injected fuel component mixes and vaporises with air, producing a peak HRR. As the HRR at TDC rises, compressed air increases the temperature of the fuel and intensifies combustion [23, 24]. HRR is controlled by continuous fuel injection, heat release from combustion, heat loss and engine cooling.

#### 5.4 Variation of Temperature

Figure 23 is illustration of temperature (T) for each crank angle is very useful for understanding the combustion process. Each of the four phases of the combustion process in the cylinder is influenced by the temperature-corresponding crank angle. The temperature variation versus crank angle for CR 14, 16.5 and 18 is shown in Figure 23, and it was found that the greatest temperatures developed at 377°, 374°, and 372°, respectively. The results suggests that NO<sub>x</sub> emissions increase as temperature rises at increasing CRs, with CR14 being the lowest.

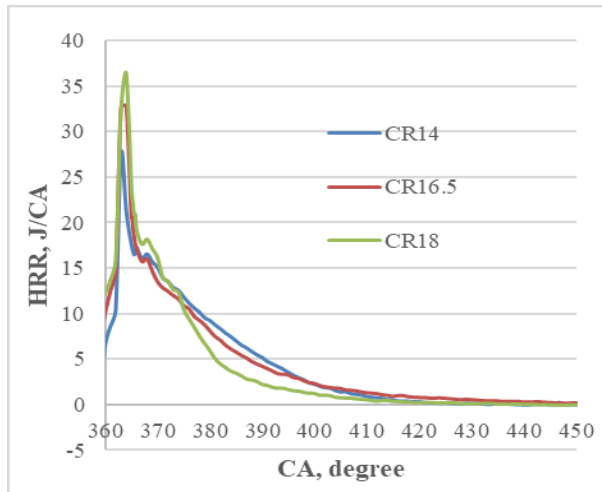


Figure 22. CFD HRR at different CRs

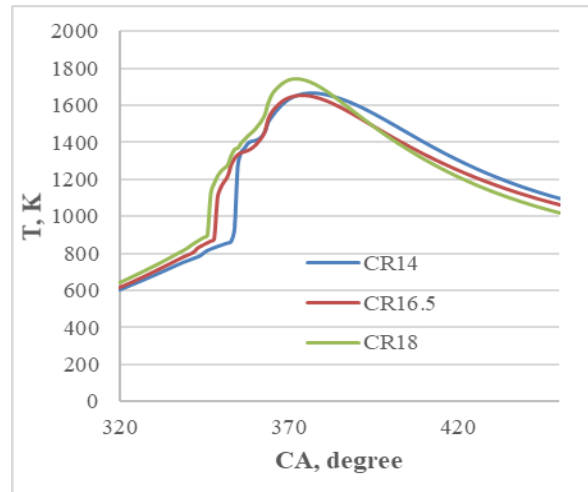


Figure 23. CFD T-CA diagram at different CRs

#### 6. Conclusions

Peak combustion pressure varies somewhat but tolerably between experimental and numerical study when CB20 fuel is used. The CFD analysis used to forecast the volume and pressure inside the combustion chamber at various CRs found that when the CR drops, the peak pressure and HRR also decrease. After combustion, the temperature in the expansion phase rises to a maximum for CR 18 and decreases with CA. For diesel engine CCs values at CR 14:1, 16.5:1, and 18:1, there is often good agreement between experimental and CFD data. As a consequence, the CCs of CI engines may be investigated using CFD analysis. For analysing the combustion of CI engines under various operating conditions, such as varying compression ratios, CFD modelling and analysis has also proven to be a viable tool. Future researchers might utilise this model to evaluate their findings while saving money and time on measuring equipment.

#### References

- [1] Abbas Alli Taghipoor Bafghi, Hosein Bakhoda, Fateme Khodaei Chegeni. Effects of Cerium Oxide Nanoparticle Addition in Diesel and Diesel-Biodiesel Blends on the Performance Characteristics of a CI Engine, *International Journal of Mechanical and Mechatronics Engineering*, Vol:9, No:8, 2015. [scholar.waset.org/1307-6892/10002117](http://scholar.waset.org/1307-6892/10002117)
- [2] M. Vijay Kumar, A. Veeresh Babu, P. Ravi Kumar, The impacts on combustion, performance and emissions of biodiesel by using additives in direct injection diesel engine, *Alexandria Engineering Journal*, Volume 57, Issue 1, 2018, Pages 509-516, ISSN 1110-0168, <https://doi.org/10.1016/j.aej.2016.12.016>.
- [3] Luka Lešnik, Jurij Iljaž, Aleš Hribnik, Breda Kegl, Numerical and experimental study of combustion, performance and emission characteristics of a heavy-duty DI diesel engine running on diesel, biodiesel and their blends, *Energy Conversion and Management*, Volume 81, 2014, Pages 534-546, ISSN 0196-8904, <https://doi.org/10.1016/j.enconman.2014.02.039>.
- [4] Shaik Mullan Karishma, Abhishek Dasore, Upendra Rajak, Tikendra Nath Verma, K. Prahlada Rao, B. Omprakash, Experimental examination of CI engine fueled with various blends of diesel-apricot oil at

- different engine operating conditions, Materials Today: Proceedings, 2021, <https://doi.org/10.1016/j.matpr.2021.02.105>
- [5] Upendra Rajak, Prerana Nashine, Abhishek Dasore, Ramakrishna Balijepalli, Prem Kumar Chaurasiya, Tikendra Nath Verma, Numerical analysis of performance and emission behavior of CI engine fueled with microalgae biodiesel blend, Materials Today: Proceedings, 2021, <https://doi.org/10.1016/j.matpr.2021.02.104>
- [6] Upendra Rajak, Prerana Nashine, Tikendra Nath Verma, Arivalagan Pugazhendhi, Performance and emission analysis of a diesel engine using hydrogen enriched n-butanol, diethyl ester and Spirulina microalgae biodiesel, Fuel, Volume 271, 2020, <https://doi.org/10.1016/j.fuel.2020.117645>
- [7] Narendra Krishania, Upendra Rajak, Prem Kumar Chaurasiya, Thokchom Subhaschandra Singh, Anil Kumar Birru, Tikendra Nath Verma, Investigations of spirulina, waste cooking and animal fats blended biodiesel fuel on auto-ignition diesel engine performance, emission characteristics, Fuel, Volume 276, 2020, <https://doi.org/10.1016/j.fuel.2020.118123>
- [8] Ganji, P.R, V. Rajesh Khana Raju, S. Srinivasa Rao. Computational Optimization of Biodiesel Combustion Using Response Surface Methodology, Thermal Science, Year 2017, Vol. 21, No. 1B, pp. 465-473. DOI: [10.2298/TSCI161229031G](https://doi.org/10.2298/TSCI161229031G)
- [9] Edwin E. Garcia Rojas, Jane S.R. Coimbra & Javier Telis-Romero. Thermo physical Properties of Cotton, Canola, Sunflower and Soybean Oils as a Function of Temperature, International Journal of Food Properties, 16:1620–1629, 2013 <https://doi.org/10.1080/10942912.2011.604889>
- [10] C.Anuradha, T. Anand Kumar, Dr. M .Lakshmi Kantha Reddy, Dr.G.Prasanthi. Effect of Injection Pressures on Emissions of Direct Injection Diesel Engine By Using CFD Simulation, IOSR Journal of Mechanical and Civil Engineering (IOSR-JMCE) e-ISSN: 2278-1684, p-ISSN: 2320-334X, Volume 13, Issue 5 Ver. V (Sep. - Oct. 2016), PP 15-19 DOI: [10.9790/1684-1305051519](https://doi.org/10.9790/1684-1305051519)
- [11] Rajesh Govindan, Dr. O.P. Jakhar, Dr. Y.B. Mathur. Computational Analysis of Thumba Biodiesel-Diesel Blends Combustion in CI Engine Using Ansys- Fluent, International Journal of Computer & Mathematical Sciences IJCMS ISSN 2347 – 8527 Volume 3, Issue 8 October 2014
- [12] Umakant V. Kongre, Vivek K. Sunnapwar, Lohara, Yavatmal. CFD Modeling and Experimental Validation of combustion in direct Ignition Engine Fueled with Diesel, International journal of applied engineering research, Dindigul Volume 1, No3, 2010
- [13] Ajay V. Kolhe, Rajesh E. Shelke, S. S. Khandare. Combustion Modeling with CFD in Direct Injection CI Engine Fuelled with Biodiesel, Jordan Journal of Mechanical and Industrial Engineering, Volume 9, Number 1, Pages 61- 66, February 2015
- [14] A. S. Zongo, G. Vaitilingom, T. Daho, Chritian Caillol, Jean-Francois Hoffman, B. Piriou, J. Valette, B. G. Segda, P. Higelin. Temperature Dependence of Density, Viscosity, Thermal Conductivity and Heat Capacity of Vegetable Oils for Their Use as Biofuel in Internal Combustion Engines, Advances in Chemical Engineering and Science, 2019, 9, 44-64 DOI: [10.4236/aces.2019.91004](https://doi.org/10.4236/aces.2019.91004)
- [15] Noor Azian Morad, A.A. Mustafa Kamal, F. Panau and T.W. Yew. Liquid specific heat capacity estimation for fatty acids, triacylglycerols, and vegetable oils based on their fatty acid composition, Journal of the American Oil Chemists' Society. September 2000, DOI: [10.1007/s11746-000-0158-6](https://doi.org/10.1007/s11746-000-0158-6)
- [16] Zaitsau and Verevkin. et al., Thermodynamics of Biodiesel: Combustion Experiments in the Standard Conditions and Adjusting of Calorific Values for the Practically Relevant Range (273 to 373) K and (1 to 200) bar, Journal of Brazilian Chemical Society, Vol. 24, No. 12, 1920-1925, 2013 <https://doi.org/10.5935/0103-5053.20130239>.
- [17] ANSYS Internal combustion engines tutorial guide, release 18.1, May 2017
- [18] V. Hariram, R. Vagesh Shangar. Influence of compression ratio on combustion and performance characteristics of direct injection compression ignition engine, Alexandria Engineering Journal (2015) 54, 807-814, DOI: [10.1016/j.aej.2015.06.007](https://doi.org/10.1016/j.aej.2015.06.007)
- [19] K. Sivaramakrishnan. Investigation on performance and emission characteristics of a variable compression multi fuel engine fueled with Karanja biodiesel-diesel blend, Egyptian Journal of Petroleum 27 (2018) 177-186. DOI: [10.1016/j.ejpe.2017.03.001](https://doi.org/10.1016/j.ejpe.2017.03.001)

- 
- [20] Narendra Krishania, Upendra Rajak, Tikendra Nath Verma, Anil Kumar Birru, Arivalagan Pugazhendhi, Effect of microalgae, tyre pyrolysis oil and Jatropha biodiesel enriched with diesel fuel on performance and emission characteristics of CI engine, Fuel, Volume 278, 2020. <https://doi.org/10.1016/j.fuel.2020.118252>
- [21] Tikendra Nath Verma, Prerana Nashine, Prem Kumar Chaurasiya, Upendra Rajak, Asif Afzal, Sakendra Kumar, Dheerendra Vikram Singh, A.K. Azad, The effect of ethanol-methanol-diesel-microalgae blends on performance, combustion and emissions of a direct injection diesel engine, Sustainable Energy Technologies and Assessments, Volume 42, 2020. <https://doi.org/10.1016/j.seta.2020.100851>
- [22] Upendra Rajak, Prerana Nashine, Prem Kumar Chaurasiya, Tikendra Nath Verma, Devendra Kumar Patel, Gaurav Dwivedi, Experimental & predicative analysis of engine characteristics of various biodiesels, Fuel, Volume 285, 2021, 119097, ISSN 0016-2361, <https://doi.org/10.1016/j.fuel.2020.119097>.
- [23] Bhaskor J.Bora, Ujjwal K.Saha, Soumya Chatterjee, Vijay Veer. Effect of compression ratio on performance, combustion and emission characteristics of a dual fuel diesel engine run on raw biogas, Energy Conversion and Management 87 (2014) 1000–1009 DOI: [10.1016/j.enconman.2014.07.080](https://doi.org/10.1016/j.enconman.2014.07.080)
- [24] H. K. Ng, S. Gan, J. H. Ng, K. M. Pang. Simulation of biodiesel combustion in a light-duty diesel engine using integrated compact biodiesel-diesel reaction mechanism, Applied Energy 102 (2013) 1275-1287. DOI: [10.1016/j.apenergy.2012.06.059](https://doi.org/10.1016/j.apenergy.2012.06.059)
- [25] Upendra Rajak , Prerana Nashine & Tikendra Nath Verma , Effect of fuel injection pressure of microalgae spirulina biodiesel blends on engine characteristics, Journal of Computational and Applied Research in Mechanical Engineering (JCARME), 2019. <https://doi.org/10.22061/JCARME.2019.4767.1578>